

# A 23 GHz Survey of GRB Error Boxes

J. N. Hewitt<sup>1</sup>, C. A. Katz<sup>1</sup>, S. D. Barthelmy<sup>2</sup>, W. H. Baumgartner<sup>1</sup>, T. L. Cline<sup>2</sup>, B. E. Corey<sup>3</sup>, G. J. Fishman<sup>4</sup>, N. Gehrels<sup>2</sup>, K. C. Hurley<sup>5</sup>, C. Kouveliotou<sup>4</sup>, C. A. Meegan<sup>4</sup>, C. B. Moore<sup>1</sup>, R. E. Rutledge<sup>6</sup>, and C. S. Trotter<sup>1</sup>

<sup>1</sup> *Department of Physics and Research Laboratory of Electronics, Massachusetts Institute of Technology*

<sup>2</sup> *NASA Goddard Space Flight Center*

<sup>3</sup> *Haystack Observatory*

<sup>4</sup> *NASA Marshall Space Flight Center*

<sup>5</sup> *Space Sciences Laboratory, University of California, Berkeley*

<sup>6</sup> *Department of Physics and Center for Space Research, Massachusetts Institute of Technology*

---

The Haystack 37-meter telescope was used in a pilot project in May 1995 to observe GRB error boxes at 23 GHz. Seven BATSE error boxes and two IPN arcs were scanned by driving the beam of the telescope rapidly across their area. For the BATSE error boxes, the radio observations took place two to eighteen days after the BATSE detection, and several boxes were observed more than once. Total power data were recorded continuously as the telescope was driven at a rate of 0.2 degrees/second, yielding Nyquist sampling of the beam with an integration time of 50 milliseconds, corresponding to a theoretical rms sensitivity of 0.5 Jy. Under conditions of good weather, this sensitivity was achieved. In a preliminary analysis of the data we detect only two sources, 3C273 and 0552+398, both catalogued sources that are known to be variable at 23 GHz. Neither had a flux density that was unusually high or low at the time of our observations.

---

## INTRODUCTION

The detection of radio counterparts to gamma-ray bursts would provide important information on the source emission mechanism, would be likely to produce more accurate position determinations, and would give a measure of the source distance through a measurement of the dispersion delay (Palmer 1993). There is, therefore, considerable interest in detecting radio counterparts to gamma ray bursts, and several searches are under way. The Haystack telescope<sup>1</sup> can make a unique contribution because of its high frequency capabilities and its ability to slew rapidly.

---

<sup>1</sup>Radio astronomy at Haystack Observatory of the Northeast Radio Observatory Consortium (NEROC) is supported by the National Science Foundation.

The Haystack telescope is optimized for operation above 1 GHz; a recently completed upgrade (Barvainis *et al.* 1993) has extended operations to frequencies as high as 116 GHz. The telescope was originally designed to track objects in low earth orbit, and high slew speeds can be tolerated. Any source position above the horizon can be reached from zenith within 30 seconds, and the complementary goals of high resolution and wide field of view may be achieved through rapid scanning of an area of the sky.

## OBSERVATIONS

Rapid continuum mapping of large fields with the Haystack telescope had not been previously attempted, and a two-week period in May 1995 was allocated to us to develop the observing techniques. At the observing frequency of 23 GHz, the beam is 1.4 arc minutes and the gain is 0.14 K/Jy. The observing frequency was chosen as a compromise between the desire to observe at as high a frequency as possible and a desire to produce a map within a reasonable period of time. The bandwidth was 160 MHz and the nominal system temperature was 140 K; the actual system temperature depended on the elevation and weather conditions (see below). Error boxes were scanned at  $0.2^\circ$ /second in right ascension, stepping in increments of  $0.00625^\circ$  in declination. Continuum data were sampled at 20 Hz, yielding Nyquist sampling in the right ascension direction and twice Nyquist sampling in the declination direction. Oversampling in declination was necessary because with the rapid scanning the telescope failed to settle to its commanded declination before beginning to scan in right ascension.

Seven BATSE error boxes and two IPN arcs were observed; the observations are summarized in Table 1. Each error box was scanned in several “slices;” and in most cases each slice was observed more than once. Observing conditions varied considerably with source elevation and as the weather changed. For presentation in Table 1 we selected just one observation of each slice; the observation selected was that with the best sensitivity.

The data were displayed and inspected in real-time during the observations and we believe we would have noted any source with flux density exceeding ten times the rms sensitivity listed in Table 1. This detection limit must be corrected for the weather-dependent opacity at 23 GHz; for the data presented here the correction is typically about 15%.

As an example of the quality of the data produced in the survey we present in Figure 1 our map of part of the error box of BATSE #3598. This map was produced by fitting a linear baseline to five-second segments of data and subtracting the fit from the central three seconds of data. The measured pixel-to-pixel rms was 0.49 Jy, consistent with the expected value of 0.51 Jy (see Table 1). Regions in which the fit was poor are evident in the map as horizontal “streaks” over a portion of a single row; occasional unsampled pixels can also be seen. Sources (here, 3C273) appear as bright regions with

TABLE 1. Journal of Observations

	Date and Time of Burst (UT)	Date of Radio Observations (UT)	Theoretical rms Sensitivity (Jy)	Size of Map
IPN3509_1	95/04/16	95/05/24	0.52	$4.4^\circ \times 0.6^\circ$
IPN3509_2	13:26:59.76	95/05/22	0.52	$4.3^\circ \times 0.8^\circ$
IPN3509_3		95/05/22	0.52	$3.7^\circ \times 1.0^\circ$
IPN3509_4		95/05/22	0.53	$2.6^\circ \times 1.0^\circ$
IPN3512_1	95/04/18	95/05/21	0.58	$1.0^\circ \times 1.5^\circ$
IPN3512_2	23:16:35.63	95/05/21	0.58	
IPN3512_3		95/05/21	0.58	
IPN3512_4		95/05/21	0.57	
IPN3512_5		95/05/21	0.59	
IPN3512_6		95/05/22	0.51	
IPN3512_7		95/05/22	0.53	
IPN3512_8		95/05/22	0.56	
IPN3512_9		Not observed		
IPN3512_10		95/05/22	0.58	
IPN3512_11		95/05/21	0.58	
IPN3512_10		95/05/21	0.58	
BATS3552_1	95/05/06	95/05/27	0.51	$5.7^\circ \times 1.3^\circ$
BATS3552_2	23:25:12.75	95/05/27	0.50	
BATS3552_3		95/05/28	0.52	
BATS3552_4		95/05/28	0.51	
BATS3552_5		95/05/28	0.50	
BATS3567_1	95/05/09	95/05/24	0.79	$6.4^\circ \times 1.1^\circ$
BATS3567_2	23:16:05.93	95/05/24	0.62	
BATS3567_3		95/05/24	0.58	
BATS3567_4		95/05/23	0.53	
BATS3567_5		95/05/24	0.57	
BATS3567_6		95/05/23	0.49	
BATS3588_1	95/05/21	95/05/23	0.68	$4.7^\circ \times 0.9^\circ$
BATS3588_2	06:59:17.29	95/05/23	0.65	
BATS3588_3		95/05/23	0.68	
BATS3588_4		95/05/23	0.65	
BATS3588_5		95/05/23	0.67	
BATS3588_6		95/05/23	0.65	
BATS3593_1	95/05/22	95/05/26	0.52	$3.4^\circ \times 0.85^\circ$
BATS3593_2	23:41:23.18	95/05/26	0.50	
BATS3593_3		95/05/31	0.53	
BATS3593_4		95/05/30	0.56	

**TABLE 1.** continued

BATS3594_1	95/05/23	95/05/27	0.53	$6.6^\circ \times 1.1^\circ$
BATS3594_2	05:39:29.07	95/05/27	0.54	
BATS3594_3		95/05/27	0.50	
BATS3594_4		95/05/28	0.65	
BATS3594_5		95/05/27	0.50	
BATS3594_6		95/05/28	0.52	
BATS3598_1	95/05/24	95/05/26	0.55	$4.2^\circ \times 1.1^\circ$
BATS3598_2	04:08:19.12	95/05/26	0.51	
BATS3598_3		95/05/27	0.52	
BATS3598_4		95/05/27	0.55	

The theoretical rms sensitivity is given by  $T_{\text{sys}}/(\sqrt{\Delta\nu\tau}G)$  where  $T_{\text{sys}}$  is the measured system temperature at the time of observation,  $\Delta\nu = 160$  MHz,  $\tau = 50$  msec, and  $G = 0.14$  K/Jy.

the extent of the beam. Further data analysis is in progress.

## RESULTS

In the preliminary analysis of the data during the observations, only 3C273 was detected; 0552+398 was noted when we examined our maps for previously known, catalogued sources. No other source was detected in the maps summarized in Table 1. 3C273 is in the error box of BATSE#3598 (see Figure 1); 0552+398 is in the error box of BATSE#3594. The data analysis is still in progress; careful examination of all radio maps and averaging of the data for boxes scanned more than once may yield further detections.

It is possible that radio-loud AGN are the sources of the gamma ray bursts. However, both 3C273 and 0552+398 are already known to be variable and neither had a flux density that was unusually high or low during the time of our observations. Therefore, there is no compelling reason to associate either with a GRB.

## FUTURE PROSPECTS

Now that the continuum mapping technique with the Haystack telescope has been demonstrated, further observations of GRB error boxes have been proposed. During this past summer, the telescope servo system was replaced. With the improved pointing control more rapid scanning of boxes should be possible, making feasible observations at higher frequencies. A new receiver

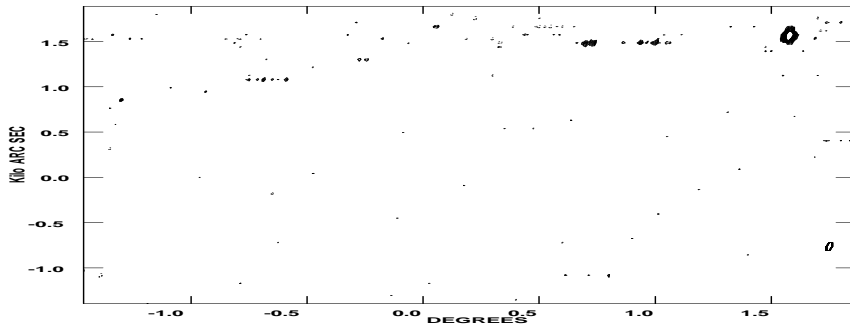


**FIG. 1.** Contour plot of map of part of the error box of BATSE#3598. The contours are -3, 3, 4, 5, 6, 7, 8, 9, 10, 11, 12, 13, 14, 15, 16, 17, 18, 19, and 20 times the root-mean-square value of the map of 0.49 Jy. The source visible in the upper right corner is 3C273.

will provide lower receiver noise at 23 GHz and allow us to observe farther from the 22 GHz water line, further increasing the sensitivity.

#### REFERENCES

1. Barvainis, R. E., Ball, J. A., Ingalls, R. P., and Salah, J. E., P.A.S.P. **105**, 1334 (1993).
2. Palmer, D. M., Ap.J. (Lett.), **417**, L25 (1993).